Catal Lett (2009) 130:79–85
DOI 10.1007/s10562-009-9890-5

Influence of Synthesis Conditions for ZSM-5 on the Hydrothermal Stability of Cu-ZSM-5

Malin Berggrund · Hanna Härelind Ingelsten · Magnus Skoglundh · Anders E. C. Palmqvist

Received: 18 August 2008 / Accepted: 4 February 2009 / Published online: 24 February 2009

Abstract The influence of syntheses parameters of zeolite ZSM-5 on the lean NO_x reduction activity and hydrothermal stability of Cu-ZSM-5 has been investigated. The hydrothermal stability of Cu-ZSM-5 was found to depend on the aluminium source used and on the presence of $Ca(OH)_2$ in the synthesis mixture for ZSM-5.

Keywords Cu-ZSM-5 · Synthesis conditions · Lean NO_x conversion · Calcium hydroxide · Hydrothermal stability · Aging · deNO_x · HC-SCR

1 Introduction

The increased interest for more fuel efficient lean combustion engines combined with increasingly stricter emission legislation continues to drive the search for lean NO_x reduction catalysts. Close to 20 years ago, copper ion-exchanged zeolite ZSM-5 was shown to have high activity for NO_x reduction under lean conditions [1, 2]. A period of large efforts to understand the properties of this catalytic system followed, but the material was found to be insufficiently stable for automotive applications [3]. The catalytic activity was lost as a result of Cu-ion migration while the zeolite framework remained less affected [3–11]. Hence, ways to increase the bonding strength of the Cu-ions to the ZSM-5 framework are of interest to improve stability of Cu-ZSM-5. Attempts to improve the stability by introduction of other cations, ion-exchanged into Cu-ZSM-5 have resulted in small or negligible improvements using, e.g. Sm, Pd, Sn, La, Ce, Ag and Co ions [9, 12–18]. In situ synthesis of ZSM-5 onto cordierite monoliths has been reported to improve zeolite crystal stability [19].

Theoretical calculations show that the interaction between the Cu-ions and the zeolite framework in the presence of water is considerably affected by the locus of the Cu-ion and the distribution of AlO_4 tetrahedra in the zeolite structure [20]. In addition, recent experimental work indicates that the aluminium distribution in the zeolite framework is affected by the aluminium source used during the ZSM-5 synthesis [21]. It might thus be possible to stabilize the Cu-ZSM-5 catalyst by modifying the parent ZSM-5 zeolite synthesis. To our knowledge, no such studies have been performed.

Previously, we showed that the aluminium source used in the zeolite synthesis affects the catalytic activity for lean NO_x reduction [22]. Here we extend the investigation of these ZSM-5 zeolite samples with a study to evaluate the effect of the parent ZSM-5 synthesis procedure on the hydrothermal stability of the Cu-ZSM-5 for NO_x reduction. Parent ZSM-5 samples are synthesised using different aluminium sources, and in addition, a varied amount of calcium hydroxide is included in the synthesis to investigate whether the presence of calcium ions in the zeolite synthesis mixture can also affect the stability of Cu-ZSM-5. The ZSM-5 samples are Cu ion-exchanged and deposited onto monoliths for NO_x reduction experiments and their hydrothermal stability is evaluated by

M. Berggrund (✉) · H. H. Ingelsten · M. Skoglundh · A. E. C. Palmqvist
Competence Centre for Catalysis, Chalmers University of Technology, 41296 Gothenburg, Sweden
e-mail: malberg@chalmers.se

comparing lean NO_x reduction efficiencies over fresh and aged samples.

2 Experimental Methods

2.1 Sample Preparation

2.1.1 Chemicals

The chemicals used in the zeolite syntheses were $Al(NO_3)_3 \cdot 9H_2O$ (98+%, Aldrich), $AlCl_3 \cdot 6H_2O$ (99%, Aldrich), tetraethyl orthosilicate (TEOS, ≥98%, Fluka), tetrapropylammonium hydroxide (TPAOH (aq), 1.0 M, Aldrich), and $Ca(OH)_2$ (puriss, Riedel-de Haën). The ion-exchange was performed using Cu(II) acetate $\cdot H_2O$ (>99%, Merck), and NH_4Cl (<99.5%, Riedel-de Haën).

2.1.2 Zeolite Synthesis

Eight different zeolite ZSM-5 samples were synthesised using the synthesis mixtures described in Table 1. For all eight syntheses the aluminium source was first dissolved in a small amount of water to which TEOS mixed with ethanol was added and the mixture was then stirred for 90 min. During this time the $Ca(OH)_2$ (when used) was dissolved in the remaining water after which it was added to the alumina-silica mixture with 30 min of additional stirring. Finally, TPAOH, was added and the total mixture was stirred for another 90 min. The mixture was transferred to an autoclave and kept at 170 °C during 170 h, after which the solid product was recovered, washed, dried and finally calcined in air at 550 °C for 5 h.

2.1.3 Ion Exchange

To prepare Cu-ZSM-5, the calcined prepared zeolite samples were treated in two different ion-exchange solutions. The products synthesised with calcium hydroxide were first ion exchanged three times with 1 M NH_4Cl solution (27 mL/g sample), for 20–24 h. Then, copper ions were introduced by ion-exchanging three times with 0.01 M copper(II) acetate solution (25 mL/g sample) at pH = 5–6 for 20–24 h. After each of the two types of ion-exchange treatments, the samples were calcined at 550 °C for 2 h. Samples prepared in the absence of calcium hydroxide were only ion-exchanged with copper.

2.2 Sample Characterisation and Evaluation

2.2.1 Characterisation

Phase identification was carried out with powder X-ray diffraction, (Siemens D5000, Cu K_α radiation, $\lambda = 1.54$ Å). Elemental composition and morphology analyses were performed using a Leo ultra 55 FEG SEM equipped with an Oxford Inca EDX system. The specific surface area of the Cu-ZSM-5 containing washcoats deposited on monoliths was determined using the BET method with N_2 sorption at 77 K (Micromeritics, ASAP 2010).

2.2.2 Catalytic Evaluation

The catalytic performance of the Cu-exchanged samples was evaluated in a continuous flow reactor over coated cordierite monoliths (20 wt% wash-coat, containing 80 wt% Cu-ZSM-5 sample and 20% silica binder, Bindzil).

Table 1 The influence of aluminium source and amount of $Ca(OH)_2$ used in the synthesis of ZSM-5 on the Cu-ZSM-5 molar composition and BET surface area obtained after ion-exchange with Cu(II) acetate

Sample	Batch composition of synthesis mixture			EDX analysis of products after Cu(II) acetate ion exchange			BET	
							m^2/g Washcoat	
	Al-source[a]	x[b]	y[c]	Si/Al_2 (SD)	Cu/Al_2 (SD)	Ca/Al_2 (SD)	Fresh	Aged
a	$AlCl_3$	0.0	51	65 (8.3)	0.9 (0.09)	0.0 (0)	289	293
b	$AlCl_3$	0.5	51	50 (7.6)	0.4 (0.06)	0.4 (0.2)	273	277
c	$AlCl_3$	1.1	50	38 (4.6)	0.3 (0.09)	0.9 (0.2)	237	256
d	$AlCl_3$	2.0	51	40 (6.8)	0.4 (0.19)	0.9 (0.4)	276	290
e	$Al(NO_3)_3$	0.0	49	53(13)	0.8 (0.31)	0.0 (0)	274	279
f	$Al(NO_3)_3$	0.5	49	40 (4.5)	0.3 (0.06)	0.6 (0.1)	269	272
g	$Al(NO_3)_3$	1.0	49	57 (29)	0.5 (0.31)	1.0 (0.2)	270	269
h	$Al(NO_3)_3$	2.0	49	42 (6.2)	0.4 (0.12)	1.1 (0.5)	283	280

The synthesis mixtures used had molar compositions x $Ca(OH)_2$:y SiO_2:Al_2O_3:19 TPAOH:2,000 H_2O:240 EtOH

[a] The type of aluminium source used in the zeolite synthesis

[b] $Ca(OH)_2/Al_2O_3$ molar ratio used in the zeolite synthesis

[c] SiO_2/Al_2O_3 molar ratio used in the zeolite synthesis

The monoliths (11.5 mm in diameter and 15 mm in length giving a volume of 1.56 mL) were placed about 4/5 into the heated zone of a horizontally mounted quartz tube reactor. Two thermocouples (Thermo-coax, K-type), axially placed in the reactor were used to measure the temperature in the reactor. The one regulating the gas temperature was placed 15 mm in front of the monolith and the other about 7 mm from the rear end of the monolith placed in one of the central monolith channels. Dry gases, NO (8% in Ar, 99.9%), O_2 (N60), C_3H_6 (4% in Ar, 99.98%) and Ar (N45), were added via separate mass flow controllers giving a dry gas feed. To introduce water, the gas flow was passed through a heated furnace (160 °C), into which preheated (120 °C) water, was injected via a capillary with an inner diameter of 0.1 mm. To analyse the outlet gas, a gas phase FTIR (Bio-Rad Excalibur FTS3000MX with a liquid nitrogen cooled Lin MCT detector and a Specac gas cell with 2 m path length) was used to quantify CO_2, CO, N_2O, and C_3H_6 and to monitor the presence of C_2H_4, formaldehyde, and NH_3 whereas an EcoPhysics (CLD 700ELht TECAN) chemiluminescence detector was used to quantify NO and NO_2. In addition, a MultiGas FTIR-instrument (MKS MG2000) was used to quantify CO_2, CO, N_2O, and C_3H_6 and to monitor the presence of C_2H_4, formaldehyde, and NH_3 for two of the samples (c and g).

The reactor tests consisted of four separate steps executed on the fresh as well as the aged Cu-ZSM-5 samples. Firstly, the sample was pre-oxidized in the reactor system during one hour at 550 °C with 8% O_2 using Ar as balance. Secondly, NO adsorption was analysed using a temperature programmed desorption (TPD) sequence. The adsorption was performed using a gas mixture containing 1,000 ppm NO, 8% O_2 and 0.4% water at 500 °C for 30 min and then during cooling to 150 °C at 7°/min. After 10 min flushing with Ar, the heating ramp started (150–500 °C, 20 °C/min) using a gas feed of 8% O_2 and 0.4% water in Ar to determine the amount of chemisorbed NO_x. Thirdly, steady-state experiments were performed at 450 °C with a gas feed containing 8% O_2, 1,000 ppm NO, 0.4% water, and six different concentrations of propene, giving a series with HC_1/NO_x molar ratios of 0, 1, 3, 5, 7 and 9. The duration of each step was 20 min. Fourthly, the samples were post-treated in oxidative environment at 550 °C, first in 1,000 ppm NO_2 for 20 min and then in 8% O_2 during one hour, using Ar as balance. The total flow in all the experiments was 1,000 mL/min (GHSV = 38 000 h^{-1}).

The gas concentrations used for the evaluation are all normalized, where [$NO_{2\ out}$] and [$NO_{x\ out}$] are divided by [$NO_{x\ in}$], whereas [CO_{out}], [$CO_{2\ out}$] and [$C_3H_{6\ out}$] (as [$HC_{1\ out}$]) are divided by [$C_3H_{6\ in}$] converted to [$HC_{1\ in}$]. The NO_x conversion is calculated as 1—the normalized [$NO_{x\ out}$].

2.2.3 Aging of Samples

After catalytic evaluation the Cu-ZSM-5 coated monolith samples were aged in the quartz tube reactor at 600 °C during 12 h in a feed of N_2 with 21% O_2 and 1% H_2O. Two of the samples were aged differently due to instrument failure. Sample d was aged in dry air at 600 °C for 12 h prior to aging the sample in the humid feed at 600 °C for 12 h. The other sample (b) was aged under harsher conditions with the temperature oscillating between 600 and 800 °C but with the same humid gas feed.

3 Results and Discussion

3.1 Sample Characterisation

A summary of the batch molar compositions of the synthesis mixtures used in the preparation of the ZSM-5 samples and the elemental compositions of the synthesised samples after Cu ion-exchange are given in Table 1. The BET measurements, presented in Table 1, show that the specific surface area of the samples was not considerably affected by the aging performed, thus eliminating structural collapse of the zeolite as the cause of possible loss in NO_x conversion.

3.2 Catalytic Evaluation

3.2.1 NO_x Conversion

In our previous study we found the Cu-ZSM-5 samples studied here to show high NO_x reduction at 450 °C [22]. Here, in Fig. 1, we present the NO_x conversion at 450 °C at two different HC_1/NO_x molar ratios, 1 and 9, over the fresh and aged Cu-ZSM-5 samples. Prior to aging, the samples showed a NO_x conversion that increased with the HC_1/NO_x molar ratio and at $HC_1/NO_x = 9$ reached values in the range 25–35% and 30–45% for the samples prepared with $Al(NO_3)_3$ and $AlCl_3$, respectively. For sample d, the aging in a dry feed was found to have a negligible effect on the NO_x conversion over the sample compared to its fresh state. Upon wet aging, the NO_x conversion decreased for all samples, and the extent of this decrease is a measure of their relative stability towards aging. The largest decrease in NO_x conversion was seen for sample e, which apparently was the least stable of the samples studied. For $HC_1/NO_x = 9$, this sample experienced a loss of about 55% of its maximum NO_x conversion, while the other samples lost 30% (f), 10% (g), 20% (h and a), and 25% (c and d), respectively (see Fig. 1). Also the more extensively aged sample, b, lost less of its NO_x conversion, about 45%, compared to sample e. In comparison with previous aging

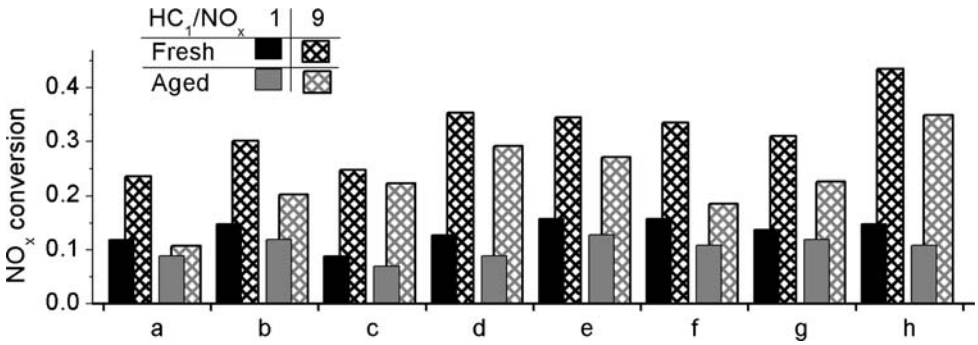

Fig. 1 The NO_x conversion at 450 °C with a HC_1/NO_x ratio 1 (■ and ■ and 9 (▩ and ▩) for Cu-ZSM-5 samples. For sample labels see Table 1. Experiments performed with fresh samples, ■ and ▩, compared with aged samples, ■ and ▩

studies [3–5, 7, 23] a low degree of aging was expected from the treatment used in this study. Hence, sample e seems to have formed relatively unstable active sites for NO_x reduction.

Since the aluminium distribution in ZSM-5 has been predicted to affect Cu-coordination and its interaction with water [20] it is interesting to know the aluminium distribution within the different zeolites. This, however, is a very complicated analytical task to perform. Using the method of correlating absorption spectra of Co-exchanged ZSM-5 samples with the distribution of AlO_4 tetrahedra Gábová et al. suggested that distinction could be made between paired and un-paired AlO_4 tetrahedra. Although it is not ascertained how relevant this method is in the current context, it is interesting to note that the use of $AlCl_3$ as aluminium source in the zeolite synthesis was reported to result in 50% paired AlO_4 tetrahedra (defined as Al–O–Si–O–Al) in the ZSM-5 structure, while $Al(NO_3)_3$ was reported to give less than 10% [21]. In combination with our study, these results support the hypothesis that an unpaired AlO_4 configuration (more than one Si atom present between the Al tetrahedra) in ZSM-5 results in less stable active sites for NO_x reduction in Cu-ZSM-5. This very intriguing conclusion suggests that different aluminium complexes are present during synthesis of the zeolite, depending on the aluminium salt used, and that local structure characteristics of these complexes are transmitted to the resulting zeolite upon its formation. An in-depth study of this topic is underway.

Furthermore, the addition of calcium hydroxide during the ZSM-5 synthesis seems to have a stabilising effect on Cu-ZSM-5 when $Al(NO_3)_3$ is used as aluminium source. All three samples synthesised with $Al(NO_3)_3$ and calcium hydroxide, f, g and h preserved their NO_x reducing ability to a higher extent than the calcium-free sample e. Since calcium remained in the Cu ion-exchanged samples it is, however, not clear whether the positive effect observed comes from calcium hydroxide-induced structural changes in the aluminium distribution of the ZSM-5 zeolite or if the remaining calcium in the samples has a stabilising effect on Cu-ZSM-5. Calcium included in the synthesis of ZSM-5 has been seen to reduce the zeolite dealumination under hydrothermal treatment in comparison to protonated ZSM-5, an effect which is also seen for copper ion-exchanged ZSM-5 [24]. In addition, calcium ion-exchanged as co-cation to copper in ZSM-5 has been reported to stabilise the square planar Cu^{2+} sites under heat treatments [25]. However, no stabilising effect of calcium was reported in a study of changes in lean NO_x reduction using propene over calcium ion-exchanged Cu-ZSM-5 upon thermal treatment [26]. The variation in these reported results is also confirmed in our study, where a stabilising effect is seen for the ZSM-5 synthesised with aluminium nitrate but not for the ZSM-5 synthesised with aluminium chloride. Thus we cannot rule out that the effect seen for the calcium-containing samples in this study depends upon incorporation of calcium in itself, rather than due to calcium hydroxide influencing the aluminium distribution during the ZSM-5 synthesis.

3.2.2 *NO Oxidation and Reduction*

In lean NO_x reduction based on the HC-SCR technique there are a number of different catalyst properties needed to achieve a high conversion of NO_x. To assess what effects the aging has that caused the decrease in NO_x conversion we evaluate the change in these properties one by one. First the effects on the NO oxidation is shown in Fig. 2 as the concentration of NO_2 at the reactor outlet, normalised to the NO_x concentration at the reactor inlet for $HC_1/NO_x = 0$. The data show that the aging performed in this study does affect the NO oxidation of the samples but in different ways depending on the sample. Aging of most samples results in a pronounced decrease in NO_2 formation 6–40%, in parity with the decrease in NO_x conversion of these samples. However, only small changes are seen for the two samples that are most affected by aging, i.e. e and b, for which a slight improvement (4%) and a small decrease (10%) in NO_2 formation is observed, respectively. Thus, no obvious direct correlation is seen between the loss of NO oxidation capacity and the loss of NO_x conversion for the sample series.

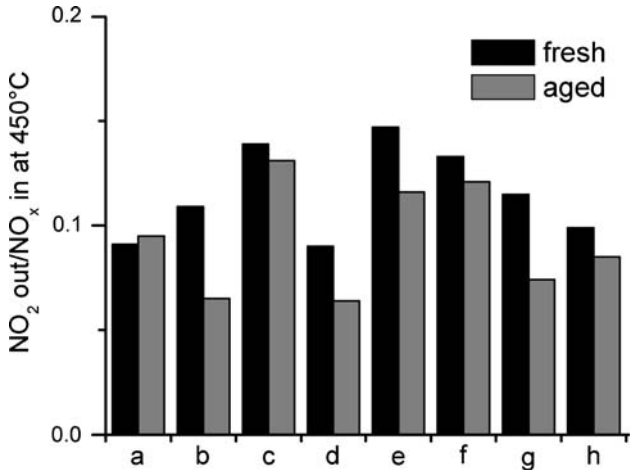

Fig. 2 Normalized NO oxidation at 450 °C in a feed of 1,000 ppm NO, 8% O_2 and 0.4% water. For sample labels see Table 1

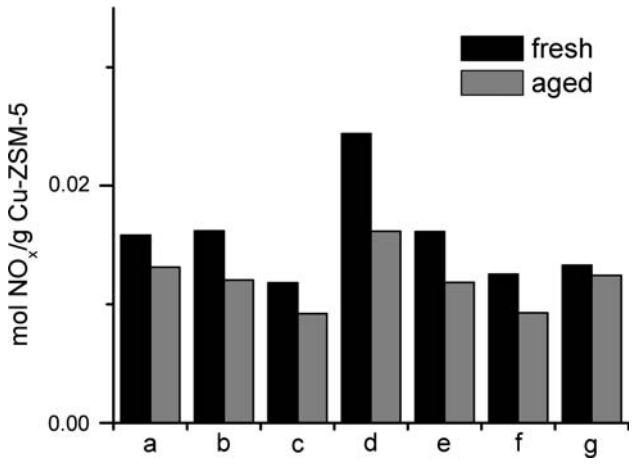

Fig. 3 Total NO_x released during the TPD performed from 150 °C to 500 °C in 8% O_2, 0.4% water and Ar balance. All NO_x stored was released as NO_2. For sample labels see Table 1

Comparing the NO_x conversion at HC_1/NO_x molar ratio 1 and 9, in Fig. 1 the total NO_x reduction is seen to increase with increased propene concentration. At HC_1/NO_x molar ratio of 1 most NO_2, which is formed in absence of propene, is consumed. Increasing the propene concentration to a HC_1/NO_x molar ratio of 9, NO_x is converted in an amount apparently exceeding that of NO_2 formed in absence of propene. Thus an apparent NO reduction can be defined as total NO_x reduced—NO_2 reduced, where the maximum NO_2 reduced is assumed to equal the NO_2 formation in absence of propene. As most NO_2 is consumed at HC_1/NO_x molar ratio of 1 the apparent NO reduction can be illustrated by the difference between the NO_x conversion at HC_1/NO_x molar ratio 1 and 9 in Fig. 1. For all samples prior to aging the apparent NO reduction increases with increasing HC_1/NO_x ratios reaching 25–45%. In contrast, for the aged samples large differences in apparent NO reduction are observed between the different samples, where notably the samples e and b have lost virtually all apparent NO reduction upon aging. The aging performed decreased the selectivity for apparent NO reduction for samples e and b, with 90 and 70%, respectively, while the other samples showed a decrease of 10–30%. There is hence a strong correlation between the decrease in NO_x conversion and the decrease in apparent NO reduction by propene. NO_x reduction has been suggested to proceed via either NO_2 formation or by NO reacting directly with propene [27–29]. Obviously we cannot determine whether the apparent NO reduction has proceeded by direct reduction of NO or via an initial oxidation to NO_2 before reduction. Nevertheless, these results clearly show that the aging of samples e and b causes loss of active sites specific for the reduction of NO_x, yet unclear if the NO_x need to be in the form of NO or NO_2, whereas sites for NO oxidation are less unambiguously affected.

3.2.3 *NO_x Storage Capacity*

It has previously been reported that a decrease in NO storage accompanies a decreased NO_x conversion [7, 8, 30]. To further evaluate the mechanisms of decreased activity for NO_x reduction the effects of aging on the NO_x storage capacity of the samples was studied. In Fig. 3 the total amount of NO_x released during the TPD experiment up to 500 °C of the samples before and after aging is shown. The decrease in NO_x storage of the samples due to the aging performed ranged from 8 to 33%, with the two most severely aged samples, e and b, showing intermediate 16 and 26% decrease, respectively. The NO_x stored was released as NO_2 only, in accordance with the literature where NO is seen to be released between 20 and 180 °C [7, 8, 31], which is below the temperature used in this TPD study. No apparent connection is thus seen between the changes in NO_x storage capacity and the NO oxidation, or the decrease in NO_x conversion, when comparing all samples. Hence, NO_x reduction sites seem to be distinct from at least some of the sites effective for NO_x storage. Possibly, the remaining calcium is active for NO_x storage since calcium oxides have been seen to store NO_2, on other supports, [32, 33]. Such an effect would reduce the correlation between the changes in NO_x storage capacity and NO_x reduction activity.

3.2.4 *Propene Oxidation Capability*

In principle, the decrease in NO_x reduction upon aging may be caused by a decreased ability of the catalyst to activate the hydrocarbon. To establish whether this was the case here, the changes in propene slip and in the formation of CO_2 and CO, were monitored and are shown in Fig. 4 for

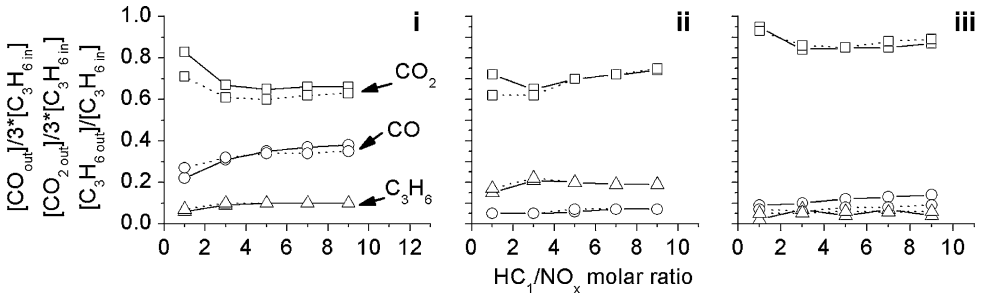

Fig. 4 Normalised concentrations of CO (-○-), CO_2 (-□-) and propene (-Δ-) at the reactor outlet during NO_x reduction with propene at 450 °C for Cu-ZSM-5 samples (*i*) e, (*ii*) g and (*iii*) a. The *solid lines* correspond to experiments with fresh samples and the *dashed lines* to experiments with aged samples. For sample labels see Table 1

the three samples, a, e and g. In these samples the oxidation of propene remains practically unaffected by aging, although some minor changes in propene slip and CO_2/CO ratio can be observed. Thus, the propene oxidation results lack obvious correlation with the decrease in NO_x reduction upon aging. Apparently, the aging does not limit the activation of propene but instead lowers the selectivity for its oxidation with NO_x.

In summary, the observed decrease in NO_x reduction upon aging over the different Cu-ZSM-5 samples does not correlate clearly with changes in their NO oxidation, propene activation or NO_x storage properties. Instead, the deactivation seems linked to the destruction of active sites specific to the reduction of NO_x, and perhaps mainly specific to the reduction of NO. In line with the reports by Gábová et al. [21] we see a dependency on the aluminium source used in the synthesis of ZSM-5. Using $AlCl_3$ in the synthesis results in a more stable Cu-ZSM-5 than the use of $Al(NO_3)_3$. It is plausible that this dependency is linked to differences in Cu coordination caused by differences in the aluminium distribution of the zeolite as suggested by Gábová et al. Furthermore, by addition of calcium hydroxide the stability of Cu-ZSM-5 prepared with $Al(NO_3)_3$ can be improved. It is, however, unclear whether this improvement is caused by a positive influence of the calcium on the aluminium distribution of ZSM-5 or by calcium acting as a stabiliser within the Cu-ZSM-5 sample where some calcium remains in the samples after Cu ion-exchange.

4 Conclusions

This study has shown that the hydrothermal stability of Cu-ZSM-5 deNO_x catalysts can be affected by choice of synthesis conditions for the parent ZSM-5. Notably, the choice of aluminium source is important, where $AlCl_3$ gives a more stable sample than the $Al(NO_3)_3$. This can be rationalised within the framework of synthesis-affected aluminium distributions in ZSM-5, which has previously been suggested to give a higher fraction of paired aluminium using $AlCl_3$ than using $Al(NO_3)_3$ [21]. It is also in accord with theoretical predictions suggesting that the copper-ions coordinate differently depending on the aluminium distribution of the zeolite [20]. In the present study, we also find that the hydrothermal stability of Cu-ZSM-5 samples prepared with $Al(NO_3)_3$ can be improved by addition of $Ca(OH)_2$ during the synthesis of the ZSM-5. Whether this improvement is of a similar origin or due to stability effects of calcium remaining after Cu ion-exchange is not clear and needs further analysis.

Acknowledgments This work has been performed within the EMFO programme, which is funded by the Swedish Agency for innovation systems, the Swedish road administration and the Swedish Environmental Protection Agency, and carried out at the Competence Centre for Catalysis, which is financially supported by the Swedish Energy Agency, AB Volvo, Volvo Car Corporation, Scania CV AB, GM Powertrain Sweden AB, Haldor Topsøe A/S and the Swedish Space Corporation. Financial support from Knut and Alice Wallenberg Foundation, Dnr KAW 2005.0055, is gratefully acknowledged.

References

1. Iwamoto M, Yahiro H, Yuu Y, Shundo S, Mizuno N (1990) Shokubai 32(6):430–433
2. Koenig A, Held W, Richter T (2004) Top Catal 28(1–4):99–103
3. Kharas KCC, Robota HJ, Liu DJ (1993) Appl Catal B Environ 2(2–3):225–237
4. Gómez SA, Campero A, Martinez-Hernandez A, Fuentes GA (2000) Appl Catal A Gen 197(1):157–164
5. Houel V, James D, Millington P, Pollington S, Poulston S, Rajaram R, Torbati R (2005) J Catal 230(1):150–157
6. Kucherov AV, Gerlock JL, Jen H-W, Shelef M (1995) J Catal 152(1):63–69
7. Matsumoto S, Yokota K, Doi H, Kimura M, Sekizawa K, Kasahara S (1994) Catal Today 22(1):127–146
8. Quincoces CE, Kikot A, Basaldella EI, Gonzalez MG (1999) Ind Eng Chem Res 38(11):4236–4240
9. Rokosz MJ, Kucherov AV, Jen HW, Shelef M (1997) Catal Today 35(1–2):65–73
10. Tanabe T, Iijima T, Koiwai A, Mizuno J, Yokotam K, Isogai A (1995) Appl Catal B Environ 6(2):145–153

11. Zhang Y, Flytzani-Stephanopoulos M (1996) J Catal 164(1):131–145
12. Chajar Z, Denton P, De Bernard FB, Primet M, Praliaud H (1998) Catal Lett 55(3,4):217–222
13. Kucherov AV, Hubbard CP, Kucherova TN, Shelef M (1997) Stud Surf Sci Catal 105B:1469–1476 (Progress in Zeolite and Microporous Materials, Pt. B)
14. Kucherov AV, Kucherova TN, Slinkin AA (1995) Stud Surf Sci Catal 94:657–664 (Catalysis by Microporous Materials)
15. Palella BI, Lisi L, Pirone R, Russo G, Notaro M (2006) Kinet Catal 47(5):728–736
16. Pârvulescu VI, Centeno MA, Grange P, Delmon B (2000) Journal of Catalysis 191(2):445–455
17. Praserthdram P, Phatanasri S, Rungsimanop J, Kanchanawanichkun P (2001) J Mol Catal A Chem 169(1–2):113–126
18. Wierzchowski PT, Zatorski LW (2002) Catal Lett 78(1–4):171–176
19. Landong L, Jixin C, Shujuan Z, Fuxiang Z, Naijia G, Tianyou W, Shuliang L (2005) Environ Sci Technol 39(8):2841–2847
20. Davidová M, Sauer J, Sierka M, Nachtigall P (2004) Abstract of the 14'th International Zeolite Conference. Cape Town, South Africa
21. Gábová V, Dědeček J, Čejka J (2003) Chem Commun (Cambridge United Kingdom) (10): 1196–1197
22. Berggrund M, Skoglundh M, Palmqvist AEC (2007) Top Catal 42/43:153–156
23. Grinsted RA, Jen HW, Montreuil CN, Rokosz MJ, Shelef M (1993) Zeolites 13(8):602–606
24. Sano T, Murakami T, Suzuki K, Ikai S, Okado H, Kawamura K, Hagiwara H, Takaya H (1987) Appl Catal 33(1):209–217
25. Kucherov AV, Shigapov AN, Ivanov AA, Shelef M (1999) Journal of Catalysis 186(2):334–344
26. Keiski RL, Raeisaenen H, Haerkoenen M, Maunula T, Niemistoe P (1996) Catal Today 27(1–2):85–90
27. Hwang IC, Kim DH, Woo SI (1996) Catal Lett 42(3,4):177–184
28. Park S-K, Park Y-K, Park S-E, Kevan L (2000) Phys Chem Chem Phys 2(23):5500–5509
29. Shelef M (1995) Chem Rev (Wash DC) 95(1):209–225
30. Tounsi H, Djemel S, Ghorbel A, Delahay G, de Menorval LC, Coq B (2004) React Kinet Catal Lett 81(1):33–40
31. Ansell GP, Diwell AF, Golunski SE, Hayes JW, Rajaram RR, Truex TJ, Walker AP (1993) Appl Catal B Environ 2(1):81–100
32. Huang HY, Long RQ, Yang RT (2001) Energy & Fuels 15(1):205–213
33. Sadykov VA, Baron SL, Matyshak VA, Alikina GM, Bunina RV, Rozovskii AY, Lunin VV, Lunina EV, Kharlanov AN, Ivanova AS, Veniaminov SA (1996) Catal Lett 37(3,4):157–162